

Phosphorus-31 Chemical Shift Anisotropies in Solid, Octahedral Chromium(0) Triphenylphosphine Derivatives

Yining Huang, Haewon L. Uhm, Denis F. R. Gilson,* and Ian S. Butler*

Department of Chemistry, McGill University, 801 Sherbrooke Street West, Montreal, Quebec, Canada H3A 2K6

Received July 11, 1996[⊗]

The ³¹P chemical shift anisotropies have been measured at 293 K for the triphenylphosphine ligands in solid pentacarbonyl(triphenylphosphine)chromium(0), Cr(CO)₅(PPh₃) (**1**), and *cis*- and *trans*-tetracarbonyl(triphenylphosphine)(thiocarbonyl)chromium(0), Cr(CO)₄(PPh₃)(CS) (**2** and **3**). The major changes in the shift tensors occur for the δ_{11} and δ_{22} components perpendicular to the Cr–P bond direction. The individual tensor components of the ³¹P chemical shifts are clearly more important than are the isotropic values in providing information on the chromium–phosphorus bonding. The crystal structure of **3** has been determined by single-crystal X-ray diffraction. The complex crystallizes in the monoclinic *P*2₁/*n* (No. 14) space group with cell constants (at 293 K) *a* = 9.558(5) Å, *b* = 15.275(2) Å, *c* = 15.341(2) Å, β = 96.66(2)°, *V* = 2225(1) Å³ and *Z* = 4; *R* = 0.069 and *R*_w = 0.067. The crystal structure of **1** has been reported previously and most of the structural features are quite similar to those for **3**. For instance, the Cr–P distances are 2.422(4) Å for **1** and 2.424(4) Å for **3**. The P–Cr–C(S) and Cr–C–S linkages in **3** are almost linear with the angles being 178.4(4) and 174.1(9)°, respectively. The most significant difference between **1** and **3** is that Cr–C(X) (X = O, S) distance *trans* to PPh₃ is appreciably shorter for the thiocarbonyl, *viz.*, 1.79(1) vs 1.845(4) Å. This shortening would be expected if CS is a much better π -acceptor ligand than is CO, as is thought to be the case.

Introduction

Phosphorus-31 NMR spectroscopy has been widely used in organometallic chemistry since the chemical shift is extremely sensitive to electronic, steric, and geometric environments of the ³¹P nuclei.¹ Upon coordination to a metal, the chemical shifts are also influenced by such factors as the bonding interaction between the phosphorus ligand and the metal, the nature and the oxidation state of the metal, the coordination number, the influence of the *trans* ligand, and the position of the phosphorus ligand within the coordination sphere. Most of the theoretical and experimental work on coordinated phosphorus compounds, however, has been limited to studies of isotropic chemical shifts in solution. Only a few investigations have dealt fully with the tensorial nature of the chemical shift interactions. The use of isotropic chemical shifts results in the loss of important information because the principal axial components are inherently more informative than are the isotropic values. For example, in some cases, a change in molecular structure may lead to a small or negligible change in isotropic shift, while the individual principal components may undergo substantial variations in opposing directions. Therefore, the individual tensor components, δ_{ii} [or in some cases, the anisotropy, $\Delta\delta = \delta_{11} - (\delta_{22} + \delta_{33})/2$], are more sensitive to the structured parameters. The first step to improve the understanding of ³¹P chemical shielding interactions is to

investigate the variation of the principal components of the shielding tensor with changes in molecular structure.

Many transition metals have quadrupole moments, and the solid-state NMR spectra can be complicated by interactions between the shift tensor, the quadrupole tensor, and the dipolar and scalar couplings.² Chromium, however, has only one isotope with spin, ⁵³Cr (*I* = –3/2), which is only 10% abundant, and so the spectra are much simpler. The results of measurements of the ³¹P shielding tensors for three chromium(0) complexes, Cr(CO)₅(PPh₃) (**1**) and *cis*- and *trans*-Cr(CO)₄(CS)(PPh₃) (**2** and **3**), are presented here, together with the X-ray crystal structure of **3** for comparison with the known crystal structure of **1**.³

Experimental Section

Triphenylphosphine (Omega Chemical Co.) and trimethylamine *N*-oxide hydrate (Aldrich Chemical Co.) were used without further purification. All solvents used were of reagent-grade quality (Aldrich Chemical Co.). The solvents were dried over sodium/benzophenone and distilled under N₂ immediately prior to use. All the synthetic procedures were performed under N₂ atmosphere in Schlenk-type apparatus and the solvents and solutions were transferred by means of syringes.

Complexes **1**–**3** were prepared as follows. A mixture of Cr(CO)₅(CS) (0.192 g, 0.81 mmol),⁴ PPh₃ (0.218 g, 0.83 mmol), and the ligand substitution promoter^{5,6} trimethylamine *N*-oxide (Me₃NO·2H₂O; 0.120 g, 1.08 mmol) in toluene (50 mL) was heated at 50 °C for 1 day. The resulting solution was allowed to cool and filtered. The solvent was removed from the filtrate under reduced pressure (Buchi rotavapor). The oily residue remaining was adsorbed onto silica gel (Merck, grade

[⊗] Abstract published in *Advance ACS Abstracts*, January 1, 1997.

(1) For example, see: (a) Lindner, E.; Fawzi, R.; Mayer, H. A.; Eichele, K.; Pohmer, K. *Inorg. Chem.* **1991**, *30*, 1102. (b) Dixon, K. R. In *Multinuclear NMR*; Mason, J., Ed.; Plenum Press: New York, 1987. *Phosphorus-31 NMR Spectroscopy in Stereochemical Analysis: Organic Compounds and Metal Complexes*; Verkade, J. G., Quin, L. D., Eds.; VCH Publishers: Deerfield Beach, FL, 1987. (c) Gorenstein, D. G. *Prog. Nucl. Magn. Reson.* **1983**, *16*, 1. (d) Meek, D. W.; Mazanec, T. J. *Acc. Chem. Res.* **1981**, *14*, 266. (e) Pregosin, P. S.; Kunz, R. W. *³¹P and ¹³C NMR of Transition Metal Phosphine Complexes in NMR Basic Principles and Progress*; Springer-Verlag: Berlin, 1979; Vol. 16.

(2) Harris, R. K.; Olivieri, A. C. *Prog. NMR Spectrosc.* **1992**, *24*, 435.

(3) Plastas, H. J.; Stewart, J. M.; Grim, S. O. *Inorg. Chem.* **1973**, *12*, 265.

(4) English, A. M.; Plowman, K. R.; Baibich, I. M.; Hickey, J. P.; Butler, I. S. *J. Organomet. Chem.* **1981**, *205*, 177. (b) Uhm, H. L. Ph.D. Thesis, McGill University, Montreal, Quebec, Canada, 1992.

(5) Albers, M. O.; Coville, N. J. *Coord. Chem. Rev.* **1984**, *53*, 227.

(6) Luh, T.-Y. *Coord. Chem. Rev.* **1984**, *60*, 255.

60, 230–400 mesh; 1.3 g) and this mixture was placed on top of a 33 × 1.7 cm silica gel chromatography column. A 1:20 ether–hexanes mixture was used to elute the reaction products from the chromatography column. Subsequent solvent removal under reduced pressure afforded a yellow solid (0.146 g). Slow recrystallization of this material from a 1:1 THF–hexanes mixture gave crystallographic-grade yellow crystals of **3** (0.64 g) and lesser amounts of compounds **1** and **2**. The identity of each complex was established by comparison of its IR [$\nu(\text{CO})$ region] and ^{31}P -NMR spectra in solution with those already in the literature.⁷ Data for **2** are as follows. IR (hexanes): $\nu(\text{CO})$ 2045 w, 1992 w, 1960 vs, 1945 w; $\nu(\text{CS})$ 1244 m cm^{-1} . ^{31}P -NMR (CDCl_3): 52.43 ppm (s). Data for **3** are as follows. IR (hexanes): $\nu(\text{CO})$ 2063 vvw, 1960 vs; $\nu(\text{CS})$ 1244 m cm^{-1} . ^{13}C -NMR (CDCl_3): 330.94 (1C, s, CS), 212.88 ppm (4C, s, CO). ^{31}P -NMR (CDCl_3): 46.18 ppm (s).

The IR spectra were recorded on a Bomem MB-100 FT spectrometer equipped with a KBr beamsplitter and a DTGS detector. The ^{13}C - and ^{31}P -NMR spectra were measured for concentrated solutions on a Varian XL-300 spectrometer. The solid-state ^{31}P -NMR spectra were obtained on a Chemagnetics CMX-300 spectrometer operating at 121.28 MHz, with cross-polarization (CP) and high-power proton decoupling. The 90° pulse width was about 2.5 μs . The CP-MAS spectra were recorded for samples packed into a bullet-type zirconia rotor (7.5 mm diameter). Typical conditions employed were as follows: recycle delay, 10 s; contact time, 2 ms; number of data acquisitions, 3000–6000. The principal values of the chemical shift tensor were determined from the spinning sideband intensities in the MAS spectra by the graphical method of Herzfeld and Berger⁸ from the CP-MAS spectra acquired at two different spinning rates. The tensor components of the ^{31}P nuclei in PPh_3 were obtained from the nonspinning spectra only, using a phase-cycled Hahn echo pulse sequence (90°– t –180°).⁹ The undistorted echo spectrum was obtained by taking a Fourier transform of the data starting at the echo maximum. All the measurements were conducted at 293 K, except that spectra of PPh_3 were also recorded at low temperature, where the sample temperature was regulated to within ± 2 K by a RKC REX-C1000 temperature controller.

The single-crystal, X-ray measurements were performed on a Rigaku AFC6S diffractometer, with graphite-monochromated Mo K α radiation. A yellow parallelepiped crystal with approximate dimensions 0.20 × 0.18 × 0.04 mm was mounted on a glass fiber. Cell constants and an orientation matrix for data collection were obtained from a least-squares refinement using the setting angles of 25 carefully centered reflections in the range 15.02 < 2 θ < 22.95°. The data collected using the ω –2 θ scan technique to a maximum 2 θ value of 50° at a scan rate of 16°/min. Of the 4353 reflections collected, 4904 were unique. After every 150 reflections, the intensities of three representative reflections were measured and these remained constant throughout the data collection. An empirical adsorption correction, using the program DIFABS,¹⁰ was applied and resulted in transmission factors ranging from 0.77 to 1.11. Corrections for Lorentz and polarization effects were also applied. The structure was solved by direct methods¹¹ with the non-hydrogen atoms being refined anisotropically. The final cycle of the full-matrix least-squares refinement, based on 1499 observed reflections [$I > 3.00\sigma(I)$] and 271 variable parameters, converged with unweighted and weighted agreement factors of $R = 0.070$ and $R_w = 0.067$. All calculations were performed using the TEXSAN-TEXRAY crystallographic software package.¹²

Results and Discussion

The shielding tensor of PPh_3 has been investigated previously, but only at room temperature, and an axially symmetric powder pattern was observed.¹³ Since the precise C_3 symmetry at the

Table 1. ^{31}P Chemical Shift Anisotropies of Selected Triphenylphosphine Derivatives^{a,b}

compound	δ_{11}	δ_{22}	δ_{33}	δ_{iso}	$\Delta\delta^h$	span ⁱ
PPh_3^c	9	9	–42	–8	26	–33
<i>d</i>	6	6	–43	–10	25	–37
$\text{Cr}(\text{CO})_5(\text{PPh}_3)$ (1)	127	80	–42	54	108	85
<i>cis</i> - $\text{Cr}(\text{CO})_4(\text{PPh}_3)(\text{CS})$ (2)	109	74	–30	52	87	139
<i>trans</i> - $\text{Cr}(\text{CO})_4(\text{PPh}_3)(\text{CS})$ (3)	101	70	–37	46	85	138
$\text{ClRh}(\text{PPh}_3)_3^e$	91	38	–59	23	102	150
	171	73	–100	50	185	271
	110	37	–52	32	118	162
<i>cis</i> - $\text{PtMe}_2(\text{PPh}_3)_2^f$	83	39	–43	26	85	126
	87	38	–38	29	87	125
<i>cis</i> - $\text{PtPh}_2(\text{PPh}_3)_2^f$	79	19	–52	15	96	131
	83	27	–49	20	94	132
<i>trans</i> - $\text{Ir}(\text{CO})\text{Cl}(\text{PPh}_3)_2^g$	105	–2	–30	24	121	135
<i>trans</i> - $\text{Pt}(\text{PPh}_3)_2\text{Cl}_2^h$	85	–7	–13	22	95	98
<i>cis</i> - $\text{Pt}(\text{PPh}_3)_2\text{Cl}_2^h$	89	–10	–41	13	115	130
	86	–18	–35	11	113	121
	58	3	–37	8	75	95

^a Values of the principal elements and isotropic shifts are in ppm, relative to external 85% H_3PO_4 . ^b Uncertainties are ± 10 and ± 5 ppm for the data obtained from the MAS and static spectra, respectively. ^c Data measured at 298 K. ^d Data measured at 133 K. ^e From ref 24. ^f From ref 23. ^g From ref 25. ^h $\Delta\delta$ defined as $\delta_{11} - (\delta_{22} + \delta_{33})/2$. ⁱ Defined as $\delta_{11} - \delta_{33}$ (see: Mason, J. *Solid state NMR* **1993**, 2, 285).

phosphorus site does not exist in the crystal lattice,¹⁴ the question arises whether averaging of the perpendicular components results from large-amplitude motions of the phenyl rings.¹⁵ A low-temperature measurement, at 133 K, was performed, which showed that the shift anisotropy and span were essentially unchanged. The measured values for the individual shift tensor elements are given in Table 1 and are in good agreement with those reported previously.¹³

The principal components of the shielding tensors and anisotropies of the ^{31}P nuclei in complexes **1–3** determined experimentally are listed in Table 1. The isotropic values of the ^{31}P chemical shifts in the solid-state for these triphenylphosphine–chromium(0) complexes are very close to the values reported previously for the complexes in solution.^{4,16} This suggests that there are probably no significant changes in the structures of these compounds on going from solution to the solid state. It is apparent from the data in Table 1 that, upon coordination to the metal, the ^{31}P anisotropies in the PPh_3 ligand become quite large (often more than tripled) compared with that of free PPh_3 . However, the values of δ_{33} change very little. The degeneracy of δ_{11} and δ_{22} is lifted and these two components are much more deshielded in the complexes than is the perpendicular component in the free PPh_3 molecule.

Details of the crystal structure determination of complex **3** are shown in Table 2. The final atomic positions and selected bond lengths and bond angles are listed in Tables 3–5, respectively. An ORTEP view of the molecule is shown in Figure 1, while the crystal packing is illustrated in Figure 2. There are remarkably few differences between the structures of **1**³ and **3**. The former crystallizes in a triclinic unit cell with $Z = 2$ compared to the monoclinic structure of **3** with $Z = 4$. The Cr–P bond distances are the same in both cases: 2.422(4) and 2.424(4) Å for the pentacarbonyl and thiocarbonyl, respectively. The average Cr–C(O) distance of the four *cis*-carbonyls, however, is longer in the thiocarbonyl complex, 1.91(1) vs

(7) Dombek, B. D.; Angelici, R. J. *Inorg. Chem.* **1976**, 15, 1089.

(8) Herzfeld, J.; Berger, A. E. *J. Chem. Phys.* **1980**, 73, 6021.

(9) Rance, M.; Byrd, R. A. *J. Magn. Reson.* **1983**, 52, 221.

(10) Walker, N.; Stuart, D. *Acta Crystallogr.* **1983**, 39A, 158.

(11) (a) Gilmore, C. J. *J. Appl. Crystallogr.* **1984**, 17, 42. (b) Beirskens, P. T. *Direct Methods for Difference Structures. Technical Report 1*; Crystallography Laboratory: Toernooiveld, 6525 Ed Nijmegen, The Netherlands, 1984.

(12) *TEXSAN-TEXRAY Structure Analysis Package*; Molecular Structure Corp.: The Woodlands, TX, 1985 and 1991.

(13) Penner, G. H.; Wasylishen, R. E. *Can. J. Chem.* **1989**, 67, 1909.

(14) (a) Daly, J. J. *J. Chem. Soc.* **1964**, 3799. (b) Dunn, B. J.; Orpen, A. G. *Acta Crystallogr.* **1991**, 47C, 345.

(15) Schaefer, T.; Sebastian, R.; Hruska, F. E. *Can. J. Chem.* **1993**, 71, 639.

(16) Grim, S. O.; Wheatland, D. A.; McFarlane, W. *J. Am. Chem. Soc.* **1987**, 89, 5537.

Table 2. Crystallographic Data for *trans*-Cr(CO)₄(CS)(PPh)₃

chem formula: C ₂₃ H ₁₅ CrO ₄ PS	fw = 470.4
lattice params	space group: P2 ₁ /n (No. 14)
<i>a</i> = 9.558 (5) Å	<i>T</i> = 298 K
<i>b</i> = 15.275 (2) Å	<i>λ</i> = 0.710 69 Å
<i>c</i> = 15.341 (2) Å	<i>ρ</i> _{calcd} = 1.402 g cm ⁻³
<i>β</i> = 95.66 (2)°	<i>μ</i> = 4.84 cm ⁻¹
<i>V</i> = 2225 (1) Å ³	<i>R</i> = 0.069 ^a
<i>Z</i> = 4	<i>R</i> _w = 0.067 ^b

$$^a R = \sum ||F_o| - |F_c|| / \sum |F_o|. \quad ^b R_w = [(\sum w(|F_o| - |F_c|)^2) / \sum w|F_o|^2]^{1/2}.$$

Table 3. Positional Parameters and *B*(eq) Values (Å²) for **3** with Estimated Standard Deviations in the Least Significant Figure Given in Parentheses

atom	<i>x</i>	<i>y</i>	<i>z</i>	<i>B</i> (eq)
Cr	0.27320(21)	0.11067(13)	0.57558(12)	3.63(9)
S	0.3210(6)	-0.0954(3)	0.6407(3)	9.8(3)
P	0.2377(3)	0.26379(21)	0.53847(20)	3.32(15)
O1	-0.0367(10)	0.0709(6)	0.5745(7)	7.2(6)
O2	0.2730(11)	0.1366(7)	0.7786(5)	7.5(6)
O3	0.5886(10)	0.1317(7)	0.5748(6)	6.7(6)
O4	0.2675(10)	0.0529(6)	0.3852(5)	5.8(5)
C1	-0.0504(14)	0.2710(9)	0.4977(9)	4.9(8)
C2	-0.1869(15)	0.2958(10)	0.5063(10)	6.1(9)
C3	-0.2145(16)	0.3552(11)	0.5660(12)	6.6(9)
C4	-0.1079(21)	0.3885(11)	0.6211(11)	7.8(10)
C5	0.0317(15)	0.3641(9)	0.6130(9)	5.5(8)
C6	0.0597(13)	0.3040(8)	0.5522(8)	3.9(6)
C7	0.1706(14)	0.3443(8)	0.3718(8)	4.9(7)
C8	0.1936(16)	0.3612(9)	0.2859(8)	5.2(7)
C9	0.3079(18)	0.3275(10)	0.2510(9)	5.7(8)
C10	0.4003(15)	0.2771(8)	0.3047(9)	5.3(8)
C11	0.3776(13)	0.2597(8)	0.3888(8)	4.4(6)
C12	0.2622(12)	0.2928(7)	0.4253(7)	3.5(6)
C13	0.3571(16)	0.4310(9)	0.5725(9)	6.0(8)
C14	0.4390(19)	0.4911(9)	0.6230(11)	7.3(10)
C15	0.5139(16)	0.4660(11)	0.6975(10)	6.6(9)
C16	0.5123(16)	0.3815(11)	0.7234(8)	6.8(9)
C17	0.4311(15)	0.3219(8)	0.6743(9)	5.4(7)
C18	0.3513(12)	0.3452(9)	0.5988(8)	3.8(6)
C19	0.3016(14)	-0.0014(8)	0.6058(8)	5.4(7)
C20	0.0792(16)	0.0902(8)	0.5723(9)	5.0(7)
C21	0.2717(14)	0.1341(8)	0.6991(9)	5.5(7)
C22	0.4706(14)	0.1245(9)	0.5751(8)	4.3(7)
C23	0.2687(12)	0.0763(8)	0.4550(8)	3.9(6)

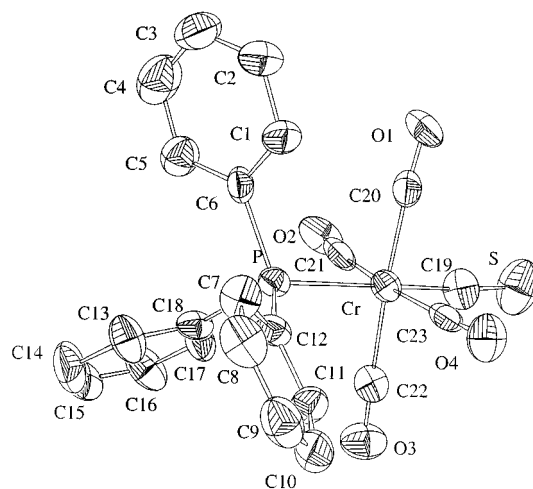
Table 4. Intramolecular Distances (Å) Involving Non-Hydrogen Atoms with Estimated Standard Deviations in the Least Significant Figure Given in Parentheses

Cr-P	2.422(4)	C(2)-C(3)	1.337(25)
Cr-C(19)	1.786(13)	C(3)-C(4)	1.35(3)
Cr-C(20)	1.875(15)	C(4)-C(5)	1.406(24)
Cr-C(21)	1.931(14)	C(5)-C(6)	1.357(18)
Cr-C(22)	1.900(14)	C(7)-C(8)	1.385(18)
Cr-C(23)	1.918(14)	C(7)-C(12)	1.376(18)
S-C(19)	1.537(13)	C(8)-C(9)	1.371(23)
P-C(6)	1.843(13)	C(9)-C(10)	1.372(22)
P-C(12)	1.833(11)	C(10)-C(11)	1.359(18)
P-C(18)	1.830(12)	C(11)-C(12)	1.389(17)
O(1)-C(20)	1.150(17)	C(13)-C(14)	1.384(21)
O(2)-C(21)	1.218(16)	C(13)-C(18)	1.374(20)
O(3)-C(22)	1.134(17)	C(14)-C(15)	1.33(3)
O(4)-C(23)	1.128(16)	C(15)-C(16)	1.351(25)
C(1)-C(2)	1.379(20)	C(16)-C(17)	1.365(19)
C(1)-C(6)	1.362(19)	C(17)-C(18)	1.358(19)

1.88(1) Å, and the former is equal to the average Cr-C(O) distance in Cr(CO)₆ [1.909(3) Å].¹⁷ The *trans*-carbonyl Cr-C(O) bond distance in **1** is 1.88(2) Å, while the corresponding Cr-C(S) distance in **3** is 1.78(1) Å. This difference implies that the π -back-bonding to the thiocarbonyl group is stronger than to the *trans*-carbonyl ligand. The average *cis*-carbonyl

Table 5. Intramolecular Bond angles (deg) Involving Non-Hydrogen Atoms with Estimated Standard Deviations in the Least Significant Figure Given in Parentheses

P-Cr-C(19)	178.4(4)	C(4)-C(5)-C(6)	120.4(13)
P-Cr-C(20)	92.5(4)	P-C(6)-C(1)	117.7(9)
P-Cr-C(21)	92.0(4)	P-C(6)-C(5)	124.2(10)
P-Cr-C(22)	90.2(4)	C(1)-C(6)-C(5)	118.2(12)
P-Cr-C(23)	92.9(4)	C(8)-C(7)-C(12)	120.9(12)
C(19)-Cr-C(20)	88.1(6)	C(7)-C(8)-C(9)	121.5(13)
C(19)-Cr-C(21)	86.6(6)	C(8)-C(9)-C(10)	117.6(12)
C(19)-Cr-C(22)	89.2(6)	C(9)-C(10)-C(11)	121.1(13)
C(19)-Cr-C(23)	88.5(5)	C(10)-C(11)-C(12)	122.2(12)
C(20)-Cr-C(21)	86.4(6)	P-C(12)-C(7)	124.1(9)
C(20)-Cr-C(22)	176.4(6)	P-C(12)-C(11)	119.3(9)
C(20)-Cr-C(23)	91.0(5)	C(7)-C(12)-C(11)	116.6(11)
C(21)-Cr-C(22)	95.9(5)	C(14)-C(13)-C(18)	120.5(13)
C(21)-Cr-C(23)	174.5(5)	C(13)-C(14)-C(15)	120.2(14)
C(22)-Cr-C(23)	86.4(5)	C(14)-C(15)-C(16)	120.2(13)
Cr-P-C(6)	113.6(4)	C(15)-C(16)-C(17)	120.0(13)
Cr-P-C(12)	115.2(4)	C(16)-C(17)-C(18)	121.6(13)
Cr-P-C(18)	118.6(5)	P-C(18)-C(13)	122.8(10)
C(6)-P-C(12)	104.4(6)	P-C(18)-C(17)	119.7(10)
C(6)-P-C(18)	102.6(5)	C(13)-C(18)-C(17)	117.5(11)
C(12)-P-C(18)	100.4(5)	Cr-C(19)-S	174.3(9)
C(2)-C(1)-C(6)	120.8(12)	Cr-C(20)-O(1)	173.8(12)
C(1)-C(2)-C(3)	121.0(14)	Cr-C(21)-O(2)	171.1(11)
C(2)-C(3)-C(4)	119.5(14)	Cr-C(22)-O(3)	179.2(12)
C(3)-C(4)-C(5)	120.1(14)	Cr-C(23)-O(4)	177.3(11)

**Figure 1.** Molecular structure of **3**. ORTEP representations are at 30% probability.

C-O distances are 1.147 Å in **1** and 1.158 ± 0.016 Å in **3**. The geometry of the tertiary phosphine ligand is the same, with average C-P-C angles of 102.7° (103.0° in the free PPh₃¹⁴) and Cr-P-C angles of 115.7° in both cases. The average P-C distance in **3** is 1.834(1) Å, i.e., close to that normally found for PPh₃ as a ligand to transition metals (1.828 Å).¹⁸ Finally, as for free PPh₃,¹⁴ one of the C-P-C angles in the coordinated PPh₃ ligand in both **1** and **3** is slightly smaller (~2°) than the other two.

A basic assumption, which is often used to discuss the tensorial orientation, is that changes in the environment of the phosphorus nucleus usually lead to changes in the values of the principal components and leave the orientation of the principal axes relatively unaffected, provided that the local symmetry remains unchanged. For example, the direction of the most shielded component, δ_{33} , lies along the Rh-P bond direction for all three ³¹P nuclei in C1Rh(PPh₃)₃.¹⁹ Although

(18) Orpen, A. G.; Brammer, L.; Allen, F. H.; Kennard, O.; Watson, D. G.; Taylor, R. *J. Chem. Soc., Dalton Trans.* **1989**, 81.

(19) Naito, A.; Sastry, D. L.; McDowell, C. A. *Chem. Phys. Lett.* **1985**, *115*, 19.

(17) Whitaker, A.; Jeffrey, J. W. *Acta Crystallogr.* **1967**, *23*, 977.

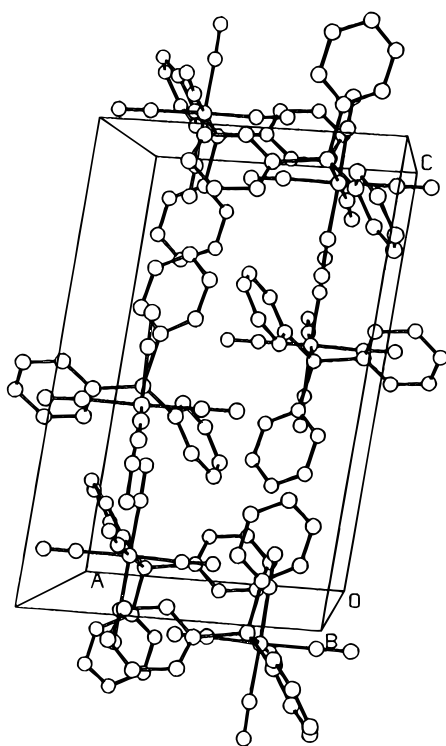


Figure 2. Crystal packing of **3**.

the X-ray studies show that the ^{31}P atoms in **1** and **3** do not lie on a true crystallographic symmetry element, the Cr–PPh₃ fragments in these complexes do have approximate C_{3v} local symmetry, and it is reasonable to assume that the δ_{33} direction is along the Cr–P bond axis. This assumption has been validated even for a number of less symmetric metal cyclic bis(phosphine) complexes.^{1a,20} The remaining two tensorial components must be in a plane perpendicular to the δ_{33} direction. Since an approximate local mirror plane at phosphorus requires one of these components to be perpendicular to the plane, the other one must lie in it. However, it is difficult to assign either δ_{11} or δ_{22} specifically to one of these two directions.

The paramagnetic components of the tensor are sensitive to changes in the current densities induced in the plane perpendicular to the tensorial direction. Since δ_{33} is directed along the Cr–P bond, the differences in the bonding between the chromium and phosphorus in complexes **1** and **3** should be reflected in the values of δ_{11} and δ_{22} . Indeed, δ_{11} and δ_{22} are more deshielded for **1** than for **3**. As mentioned earlier, the X-ray diffraction studies have shown that the structures of **1** and **3** are closely similar and do not provide any information that might explain the differences in the chemical shift tensor components.

The CS ligand is considered to be a much better π -acceptor than is CO,²¹ and removes electron density from both the Cr and P atoms, especially when the latter are *trans* to CS. On this basis, more deshielded values of δ_{11} and δ_{22} would be expected for complex **3** than for **1**, but the experimental

observations are exactly the opposite. In transition metal–phosphorus chemistry, PPh₃ is generally considered to be a poor π -acceptor ligand. However, Wovkulich and co-workers²² have demonstrated recently that the π -bonding between Cr and PPh₃ is quite significant for Cr(CO)₄(PPh₃)L complexes. Since the PPh₃ ligand competes for electron density with the ligand *trans* to it, the importance of the π -bonding will depend on the nature of the ligand L. The π -bonding between PPh₃ and Cr is more important when L is a strong σ -donor, and less so if L is a good π -acceptor. Therefore, since CS is a better π -acceptor ligand than is CO, the π -back-bonding interaction between PPh₃ and Cr should be relatively stronger in **1** compared to that in **3**. Consequently, the larger ^{31}P shielding frequency found for **1** compared to that for **3** suggests a larger anisotropy of electronic density distribution around the phosphorus, in particular, in the Cr–P direction, due to the slightly stronger π -bonding in **1**. The more deshielded δ_{11} and δ_{22} components may also arise from slight differences in the paramagnetic contributions from low-lying Cr–P $\sigma \rightarrow \pi^*$ -transition energies.

The shielding tensor values for several transition metal-triphenylphosphine complexes are also listed in Table 1. While the anisotropy ($\Delta\delta$) for complex **3** (85 ppm) is slightly lower, that for complex **1** (108 ppm) is comparable to the 121 ppm value for *trans*-Ir(CO)Cl(PPh₃)₂²³ and those for the two PPh₃ ligands *trans* to each other in ClRh(PPh₃)₂ (102 and 118 ppm), but they are substantially smaller than the 185 ppm anisotropy for the PPh₃ ligand *trans* to Cl in ClRh(PPh₃)₃.¹⁸ Upon complexation to a metal, the δ_{33} values for all the complexes listed, except for the PPh₃ ligand *trans* to Cl in ClRh(PPh₃)₃, do not vary markedly from the δ_{00} value in free PPh₃. The δ_{11} and δ_{22} components are most affected by metal–ligand bond formation, and the degeneracy of these components is always lifted upon complexation. The values of these two components also depend on the nature of the metal. In conclusion, δ_{11} and δ_{22} are particularly sensitive to the bonding between the metal and the PPh₃ ligand. The individual tensor components of the chemical shift are more informative than are the isotropic values in attempting to understand the nature of the metal–ligand bonding.

Acknowledgment. This research was supported by grants from the NSERC (Canada) and the FCAR (Québec). Y.H. thanks McGill University for the award of a Faculty of Graduate Studies and Research Fellowship. The assistance of Drs. F. Morin and J. Britten in the X-ray diffraction work and solid-state NMR measurements, respectively, is gratefully acknowledged.

Supporting Information Available: Tables for the X-ray structural determination of **3**, including details of the data collection, anisotropic thermal parameters, hydrogen atom parameters, and torsion angles (5 pages). Ordering information is given on any current masthead page.

IC960816U

(20) Lindner, E.; Fawzi, R.; Mayer, H. A.; Eichele, K.; Hiller, W. *Organometallics* **1992**, *11*, 1033 and the references therein.

(21) Butler, I. S. *Acc. Chem. Res.* **1977**, *77*, 313.

(22) Wovkulich, M. J.; Atwood, J. L.; Canada, L.; Atwood, J. D. *Organometallics* **1985**, *4*, 867.

(23) Randall, L. H.; Carty, A. J. *Inorg. Chem.* **1989**, *28*, 1194.

(24) Harris, R. K.; McNaught, I. J.; Reams, P. *Magn. Reson. Chem.* **1991**, *S60*, 29.

(25) Power, W. P.; Wasylishen, R. E. *Inorg. Chem.* **1992**, *31*, 2176.